

## Segmentation of Retinal Anatomical Structures using Morphological-based Thresholding

A.Arjuna <sup>a</sup>, Dr.R.Reena Rose <sup>b</sup>

<sup>a</sup> Research Scholar, Department of Computer Applications, St. Xavier's Catholic College of Engineering, Nagercoil, India.

<sup>b</sup> Assistant Professor, Department of Computer Applications, St Xavier's Catholic College of Engineering, Nagercoil, India.

**Abstract:** A Normal retina has anatomical structures namely optic disc and retinal vessels. An abnormal retina consists of these anatomical structures as well as pathological structures which are red and bright lesions. The proper segmentation of the retinal anatomical structures is essential for the effective diagnosis of diseases like glaucoma, diabetic retinopathy, cerebral diseases, etc. Because glaucoma affects the optic disc and other diseases harm the blood vessels. With the help of efficient segmentation of optic disc and vessels, we can easily diagnose these diseases. For this reason, here we propose a technique of morphological-based thresholding which segments the optic disc and retinal blood vessels exactly. With the help of a publicly available database namely the High-Resolution Fundus (HRF) database, this proposed method is validated. This database consists of 45 images which are grouped into three sets. For every set of images, we obtain the measures of sensitivity, specificity, and accuracy. For optic disc segmentation, we achieve the average of 0.8837, 0.9958, and 0.9932 in sensitivity, specificity, and accuracy respectively for the three sets of HRF databases. And for the vessel segmentation, we achieve an average of 0.7181 sensitivity, 0.9693 specificity and 0.9573 accuracy. And these results show that the proposed technique yields the better performance than the existing one in the literature.

**Keywords:** retina, anatomical structures, pathological structures, optic disc, vessels.

### 1. Introduction)

Retina is the light sensitive tissue which senses the light from the object and transfers it to the brain through the optic nerve to recognize the object. The visual sense of retina is dependent on retinal anatomical structures. Optic disk (OD) and the blood vessels are referred as the major retinal anatomical structures of the eye. The retinal vessels have similar characteristics of cardio vessels and cerebral vessels. The abnormalities in the blood vessels and the optic disc tend to the retinal diseases like cataract, diabetic retinopathy, glaucoma, and age-related macular degeneration [5]. Regular periodic examination of eyes prevents from the blindness caused by the retinal diseases. According to the survey, there are 65 lakh cataract surgeries are done in every year [10]. In India, 8-10% of people among the total population are affected by the diabetes. They have the chance for being affected by the retinal diseases such as diabetic retinopathy, hypertensive retinopathy etc. [7]. Cerebral vessel abnormalities such as stroke and other diseases show the sign as the retinal vessel abnormality. The manual analysis of digital fundus images about the anatomical structures is the tedious, time-consuming process for the ophthalmologists. Hence, it is necessary to develop an automated telemedicine system for segmenting the retinal structures such as optic disk and retinal blood vessels. Figure 1 shows the normal healthy retinal color fundus image.

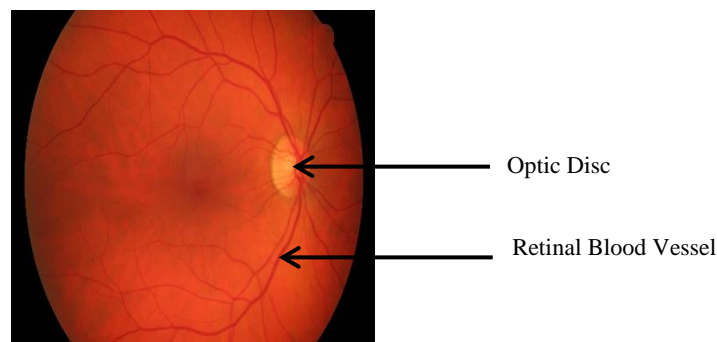


**Figure. 1:** Healthy Retinal Fundus Image

Optic disc is the bright region of the retina. It appears with the high intensity and in circular shape. The position of the optic disc may vary for image to image due to Field of View (FOV) of fundus camera at the time of image acquisition. Computerized diagnosis of retinal diseases like glaucoma and cataract and proliferative

diabetic retinopathy (PDR) needs proper automatic segmentation of the optic disk. In the glaucoma affected OD, the optic disk and the optic cup ratio become small, since the optic cup expands to the surface of optic disk. In PDR affected OD, new small blood vessels are formed inside the optic disc [4]. When protein forms in the lens, it blurs the vision. This is called cataract. Normally cataract appears in the people above the age of 40 [9].

Blood vessels are appeared as dark red in color. Some fine vessels may not be clear for the normal human eyes. Ophthalmologists cannot clearly recognize the small vessels with naked eyes. The automatic segmentation of blood vessels makes clear difference between the fine vessels and retinal background. It tends to ease diagnose of the diseases like hypertension etc.

## 2. Related Work

Since the increasing need of the automatic segmentation of the retinal structures, many researches propose different techniques to segment the retinal structures.

Zahoor et al [23] propose a series of techniques which use the morphological operations and circular hough transformation for OD localization followed by polar transform based adaptive thresholding for the segmentation. Though this technique provides higher accuracy in fast, its results are based on the illumination of optic disk. Zhang et al [24], propose a framework of light weight cascade of CNN for OD segmentation. Minimum numbers of training parameters are used for this method. But this method is complex in terms of computational task. Dulanji et al [13], use the thresholding technique after preprocessing with CLAHE and median filter on the red channel. But the red channel has less information than the green channel. Palanivel Rajan [15] use the simple thresholding technique on the greyscale conversion of the original RGB color retinal image for blood vessel and optic disc segmentation. Raja et al [17], use the convolution neural network technique to segment the retinal blood vessels. It is the supervised learning method which need training and testing. He use 90% data for training and 10% for testing. Prakash et al [19], propose the modified region growing technique for segmentation of the OD and retinal blood vessels and morphological operations are used for smoothing of segmented regions. Wisaeng et al [22], propose the series of techniques such as morphological closing, dilation, thresholding, watershed algorithm, sobel edge detection for segmentation of OD. Even if it gives better results, it is the complex and large processing task. Yi Lin et al [12] propose the deeply supervised and smoothly regularized network technique for retinal vessel segmentation. Even it provides better results, since it is supervised learning method, it requires training and testing data. Budai et al [4] present the multi resolution method, Ramakrishnan et al [14] propose the framework of the hybrid vessel segmentation algorithm which includes the morphological operations, bottom-hat transform, multi-scale vessel enhancement, image fusion operations. Odstrcilik et al [14] use the match filter technique and minimum error thresholding technique to extract the complete vessel tree. The above three authors validate their techniques on the new HRF datasets in which the results can be improved further by applying less computational techniques. Jasem et al [1] propose a hybrid segmentation technique of mathematical morphology and adaptive fuzzy thresholding. The author uses a single novel system to segment the retinal vessels and OD in parallel. Gonzalez et al [6] use the graph cut method for blood vessel segmentation and they use two consequent steps for OD segmentation. Markov Random Field method is used to remove the blood vessels from the OD regions and compensation factor method to segment exact OD region. Gagan et al [25] propose a spline based active contour method for OD segmentation.

Normally optic disc and retinal blood vessels detection and extraction system uses separate framework or the supervised machine learning techniques. Supervised machine learning techniques needs labeled data for training. Based on this training, the vessels and optic disc are segmented. This training also needs some texture, shape, intensity features for analysis which is time consuming process. The accuracy of the system is based on the selected features. And also, all the anatomical structures cannot be segmented through one system. To overcome these limitations, we propose the following simple morphological based thresholding technique to segment the optic disc and retinal vessels. We justify this technique because of its easiness and less time-consuming procedure.

This paper is organized as follows: The proposed methodology is explained in section 3. Section 4 talks about the results of the proposed methodology. Conclusion is described in Section 5.

## 3. Methodology

The proposed work of segmenting the retinal anatomical structures is mainly focused on extracting the optic disc and the blood vessels using morphological based thresholding technique with less computation cost. The following sequences of processing steps are done to segment the retinal structures and their results are analysed using the public HRF database. Figure 2 represent the overall system architecture

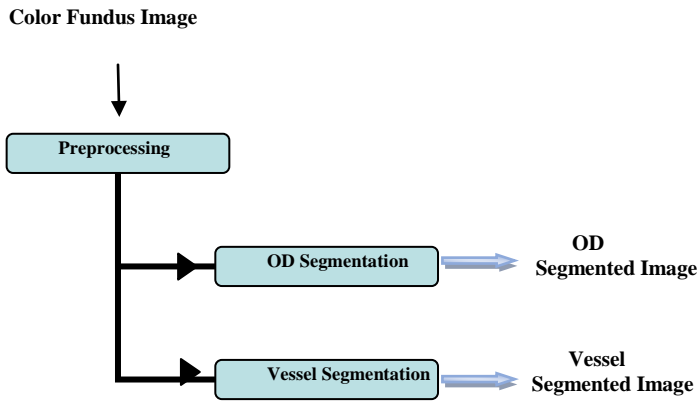


Figure. 2: Overall System Representation

### 3.1 Preprocessing

The first phase of retinal structures segmentation is the preprocessing. Normally digital fundus photographing technique is used to take the photograph of fundus images. The images taken by this technique have some clarity issues due to the focusing light of the camera [19]. So the image must be processed to enhance its clarity before segmentation. The Figure 3 shows the steps involved in the preprocessing.

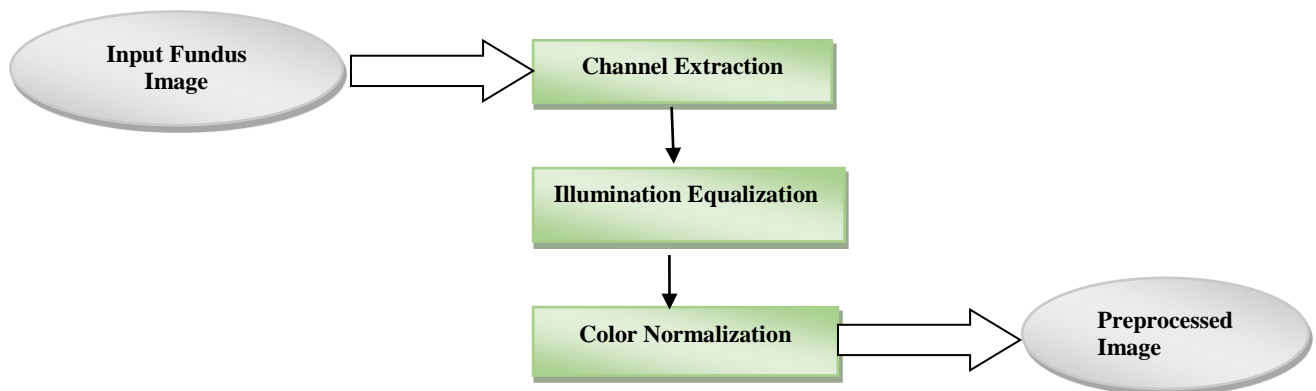
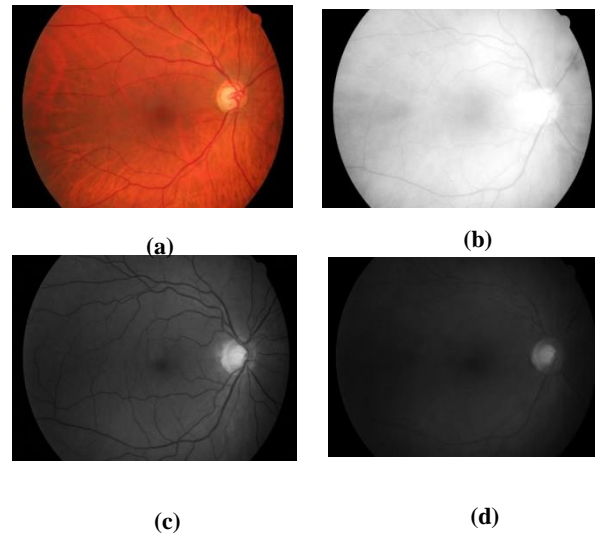


Figure. 3: Preprocessing phase

#### 3.1.1 Channel Extraction

Our automatic computer aided system takes the color fundus image as the input. Normally all color images have three color channels. They are red, green and blue color channels. Though our input fundus image also has three color channels, we take only green channel for the processing. Since the contrast between the blood vessels, optic disc and retina is very high, the green channel is suitable for the segmentation of retinal structures [11]. Figure 4 shows the three-color channels of a sample color fundus image. From the figure, it is understood that the green channel can yield good contrast for the retinal structures comparing with other two-color channels.



**Figure. 4 :** (a) Color Fundus Image, (b) Red Channel, (c) Green Channel, (d) Blue Channel

### 3.1.2 Illumination Equalization

Vignetting effect which occurred due to the improper focusing light during image acquisition, can be removed by the illumination equalization [2].

The image size is different for different data sets. For real time, the image taken by the fundus camera cannot be the same size. To generalize it, we set the image size as  $480 \times 640$ . To equalize the illumination, we use the following equation.

$$I_{ie} = I_f - I_g + \mu_g \quad (1)$$

Here,  $I_{ie}$  represents the illumination equalized image. The original green channel is represented as  $I_g$  and  $\mu_g$  represents the mean value of the original green channel.  $I_f$  is the mean filtered image with the maximum window size of  $63 \times 63$ . The window size is set experimentally.

### 3.1.3 Color Normalization

The color of the retina image is set into the standardized color range. For that, we stretch and clip the histograms of illumination equalized image ( $I_{ie}$ ) into the range  $\mu \pm 3\sigma$  [20].  $\mu$  and  $\sigma$  represents the mean and standard deviation of the image. This technique enhances the contrast of the retinal structures. It darkens the dark regions and lightens the light regions. The color normalized image is represented as  $I_{cn}$  in Figure 5.

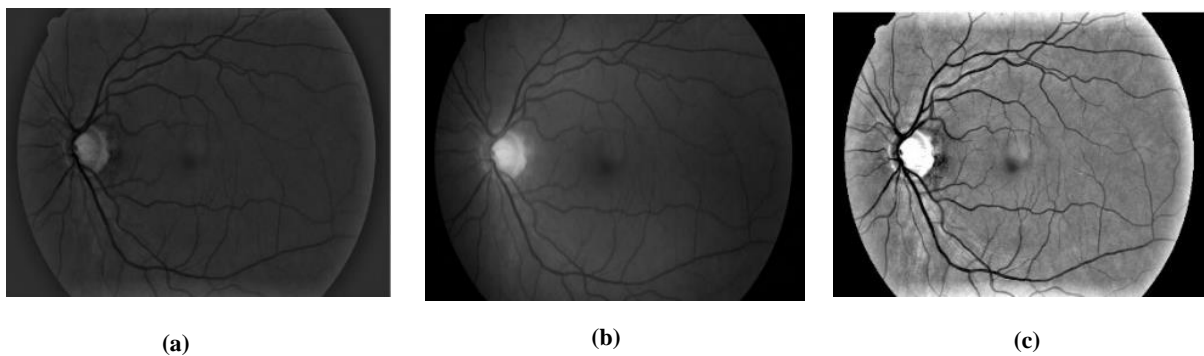


**Figure. 5:** Preprocessing. (a)  $I_g$ , (b)  $I_{ie}$ , (c)  $I_{cn}$

### 3.2. OD Segmentation

Exact Optic disc detection and segmentation is necessary for detecting the optic disc-based diseases like glaucoma, cataract etc. The overall segmentation process of the optic disc is shown below in Figure 6. The proposed technique of the optic disc segmentation is simple and easy task. It has the following processing steps.

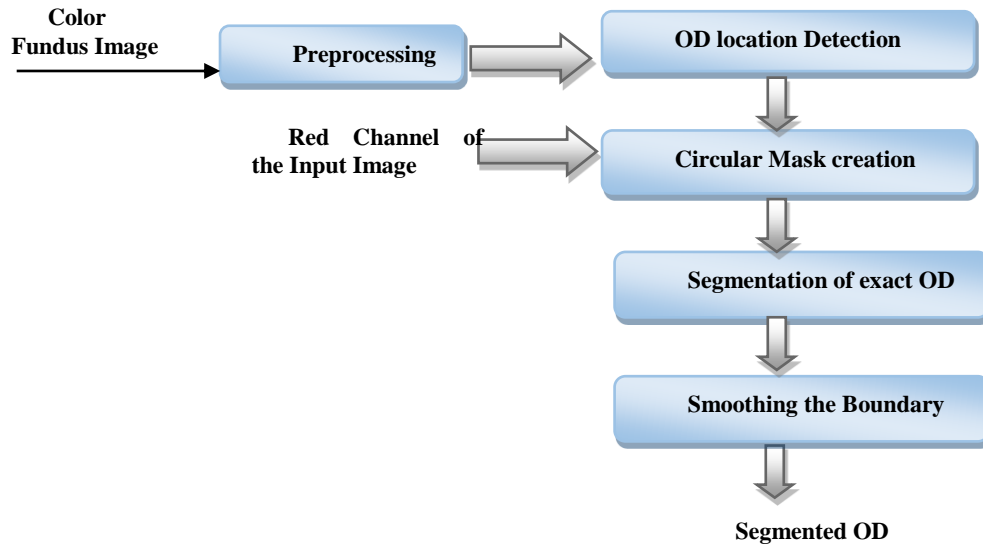


Figure. 6 : Block Diagram of Optic Disc Segmentation Technique

#### 3.2.1 Optic Disc Localization

When compared with other regions in the fundus image, optic disc has the maximum intensity [10]. So, the exact location of the optic disc is selected by using the thresholding technique. The maximum intensity of the image is taken as the threshold. Maximum intensity pixels are labeled as 1 and others as 0. Resultant image is the binary image with bright regions as white and background as black. In normal retinal images, only the optic disc has the higher intensity.

However, in diabetic retinopathy (DR) and diabetic macular edema (DME) affected retinal images, pathological structures like exudates also have higher intensity. But the optic disc has maximum area, comparing with the pathological structures. Hence, the optic disc regions can be located based on the area and the field of view (FOV) of the fundus image.

#### 3.2.2 Circular Mask Creation

Connected component analysis (CCA), is the major task in image processing for binary image analysis. Here we perform CCA in the optic disc region extracted image for finding the approximate centre of the optic disc region. Using this CCA, major and minor axis length of the optic disc regions are also calculated.

By using this center and the major axis length, the binary mask for the optic disc region is formed. The size of the mask is approximately equal to the size of the optic disc and has the radius of 10 pixels greater than the major axis length. This mask just locates the OD ROI region. To extract the OD ROI region, this mask is overlapped on the red channel of the fundus image.

#### 3.2.3 Segmentation of Exact OD

The overlapped red channel with the inverted binary mask shows exact optic disc region. Because of the high luminous effect on the red channel, the major big vessels are not visible inside the optic disc in red channel. Hence, it is easy to segment the exact optic disc region in the red channel is simply easy task. Segmentation is carried out using thresholding technique with the threshold value as 0.92. After that, the noisy regions having small areas are closed using morphological closing operation.

### 3.2.4 Smoothing the Boundary of OD

Morphological dilation operation with ‘disk’ shaped structuring element is used to smoothen the boundary of the segmented optic disc region. After smoothing we can get the exact optic disc region. The output of each step of OD segmentation process is shown in the below Figure 7.

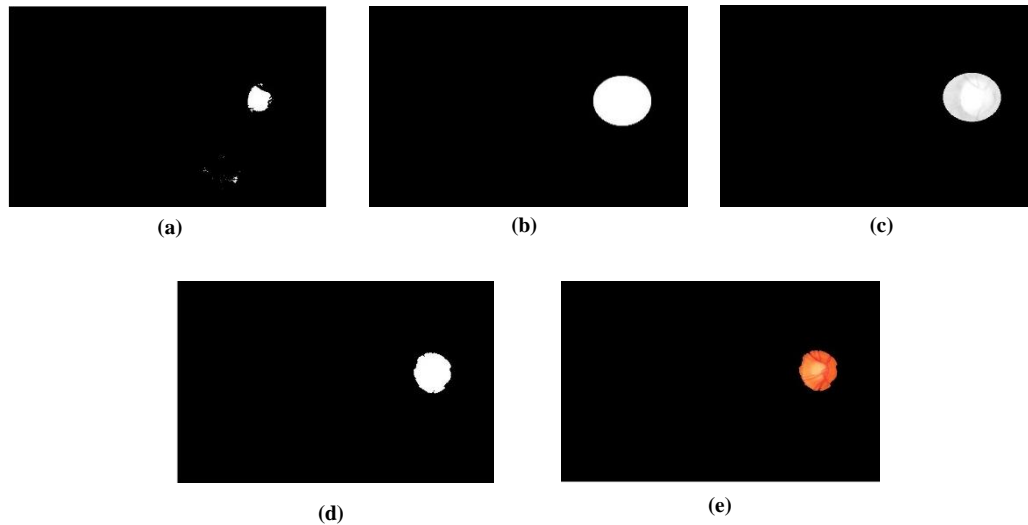


**Figure. 7 :** OD Segmentation. (a) Located OD, (b) Circular Mask, (c) Circular Mask with red channel, (d) Segmented OD in binary image, (e) Segmented OD

### 3.3. Retinal Vessel Segmentation

Retinal vessels are of dark intensity. Hence, to separate the vessels from the background, estimation of the background has to be done as the initial step. It is done by applying median filter [15] with the experimentally estimated window size of 15. This process is carried out in the pre-processed green channel of the fundus image.

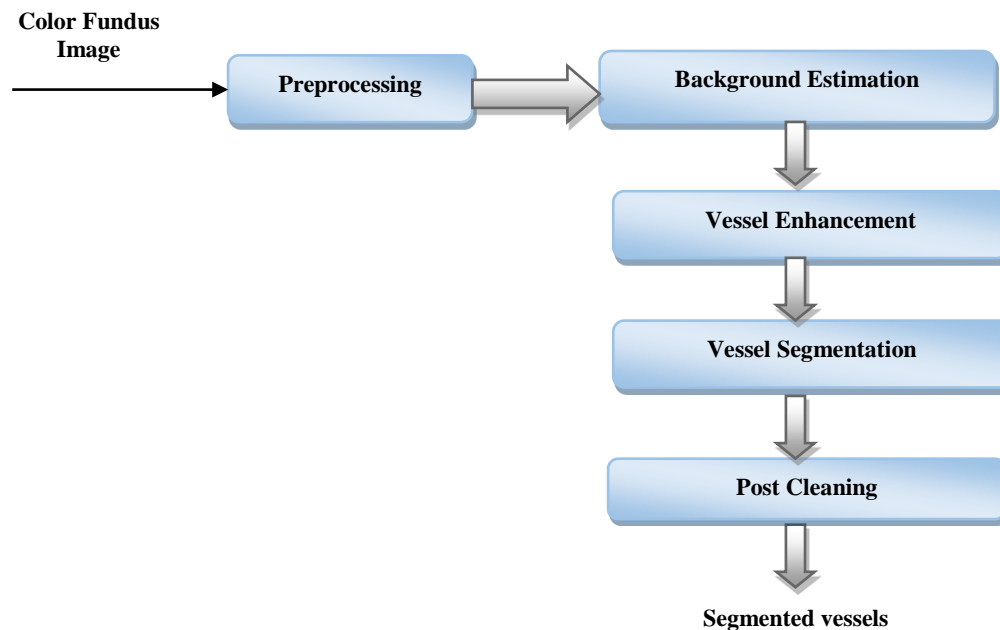


**Figure. 8 :** Block Diagram of Retinal Vessel Segmentation Technique

### 3.3.1 Background Estimation

Retinal vessels are of dark intensity. Hence, to separate the vessels from the background, estimation of the background has to be done as the initial step. It is done by applying a median filter [15] with the experimentally estimated window size of 15. This process is carried out in the pre-processed green channel of the fundus image.

### 3.3.2 Vessel Enhancement

This is done by subtracting the filtered image from the preprocessed green channel of the image. The resultant image displays dark regions as bright. This bright area represents only the blood vessels in the normal image, however, in DR affected fundus images, it also represents red lesions.

### 3.3.3 Vessel Segmentation

The enhanced blood vessels are segmented by using following eqn.2 .

$$vs(x,y) = \begin{cases} 255 & \text{if } b(x,y) > 15, \\ 0 & \text{otherwise} \end{cases} \quad (2)$$

Here,  $vs(x,y)$  represent the vessel segmented image, and  $b(x,y)$  represents the vessel enhanced image.

As the result, the dark regions are displayed as white and others are displayed as dark.

### 3.3.4 Post Cleaning

After applying thresholding, the thresholded image  $vs(x,y)$  contains not only blood vessels, but also the other dark regions such as red lesions and other dark retinal background as noise. To remove these noise, Connected Component Analysis (CCA) is performed. Using this CCA, the regions having area below 200 pixels are neglected [12]. The final output image have the segmented retinal blood vessels.

Outputs of the final retinal blood vessel segmentation phase are shown in the Figure 9.

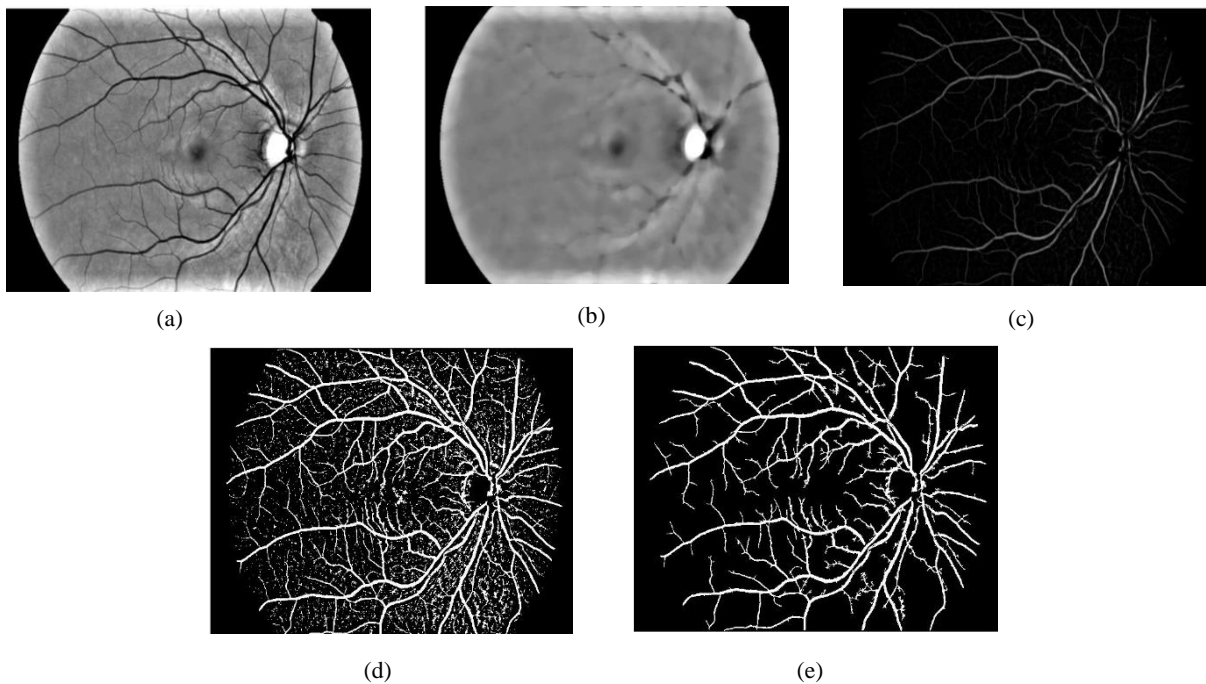


**Figure 9:** Retinal Vessel Segmentation: (a) Green Channel, (b) Background estimated green channel, (c) Enhanced Blood Vessel, (d) Segmented vessels with noise, (e) Exact Segmented Vessels

## 4. Results and Evaluation

### 4.1 Material

**HRF Database:** It stands for High Resolution Fundus Image Database [11]. This database consists of 45 retinal fundus images. These 45 images are classified into three sets. The first one is the healthy image set which contains retinal images the healthy people who do have not pathological symptoms. The second set contains the retinal fundus images having the signs of diabetic retinopathy. The third consists the retinal images of the glaucoma-affected patients.

All these images are taken with the help of a mydriatic fundus camera CANON CF-60 UVi equipped with CANON EOS-20D digital camera with a field of view (FOV) of 60 degrees. Before taking photographs, the standard mydriatic drops are used to dilate the patient's pupil. Hand-labeled ground truth images for the retinal blood vessels in a binary format are attached to this database

## 4.2 Evaluation

Ground truth images for the optic disc segmentation are manually created in binary format. Both the ground truth images of blood vessel and optic disc segmentation are compared and evaluated with the output images by pixel wise.

The following metrics are used for evaluating the proposed methods.

$$\text{Sensitivity} = \frac{TP}{TP + FN}$$

$$\text{Specificity} = \frac{TN}{TN + FP}$$

$$\text{Accuracy} = \frac{TP + TN}{TN + FP + TP + FN}$$

TP stands for True Positive – Number of pixels correctly segmented as retinal structures.

FP stands for False Positive – Number of pixels incorrectly segmented as retinal structures.

TN stands for True Negative – Number of pixels correctly segmented as background pixels.

FN stands for False Negative – Number of pixels incorrectly segmented as background pixels.

Both segmentation techniques are evaluated separately on the three set images of HRF database

### 4.2.1 Evaluation of OD segmentation Technique

Here three set of images are evaluated separately with their equivalent hand labeled ground truth images and their results are listed in the below tables.

**Table 1.** Performance of OD segmentation for healthy images of HRF dataset

Image No.	Measures		
	<i>Sensitivity</i>	<i>Specificity</i>	<i>Accuracy</i>
<b>1_h</b>	0.8208	0.9962	0.9935
<b>2_h</b>	0.8009	0.9971	0.9945
<b>3_h</b>	0.9842	0.9907	0.9906
<b>4_h</b>	0.8108	0.9903	0.9876
<b>5_h</b>	0.7764	0.9952	0.9920
<b>6_h</b>	0.8547	0.9973	0.9905
<b>7_h</b>	0.8014	0.9956	0.9897
<b>8_h</b>	0.8409	0.9971	0.9903

Image No.	Measures		
	<i>Sensitivity</i>	<i>Specificity</i>	<i>Accuracy</i>
<b>9_h</b>	0.9957	0.9872	0.9873
<b>10_h</b>	0.9104	0.9997	0.9986
<b>11_h</b>	0.8909	0.9996	0.9945
<b>12_h</b>	0.8679	0.9969	0.9953
<b>13_h</b>	0.8666	0.9970	0.9954
<b>14_h</b>	0.8279	0.9996	0.9945
<b>15_h</b>	0.8474	1.0000	0.9961
<b>Average</b>	<b>0.8598</b>	<b>0.9960</b>	<b>0.9927</b>

**Table 2.** Performance of OD segmentation for DR affected images of HRF dataset

Image No.	Measures		
	<i>Sensitivity</i>	<i>Specificity</i>	<i>Accuracy</i>
<b>1_dr</b>	0.8149	0.9979	0.9892
<b>2_dr</b>	0.8580	0.9985	0.9946
<b>3_dr</b>	0.8771	0.9997	0.9957
<b>4_dr</b>	0.9226	0.9992	0.9984
<b>5_dr</b>	0.8246	0.9986	0.9966
<b>6_dr</b>	0.7413	0.9944	0.9907
<b>7_dr</b>	0.8385	0.9998	0.9948
<b>8_dr</b>	0.9436	0.9912	0.9907
<b>9_dr</b>	0.9770	0.9887	0.9885
<b>10_dr</b>	0.8683	0.9975	0.9933
<b>11_dr</b>	0.8937	0.9984	0.9929
<b>12_dr</b>	0.8444	0.9984	0.9933
<b>13_dr</b>	0.8081	0.9924	0.9898
<b>14_dr</b>	0.8298	0.9978	0.9956
<b>15_dr</b>	0.8317	0.9973	0.9957
<b>Average</b>	<b>0.8582</b>	<b>0.9967</b>	<b>0.9933</b>

**Table 3.** Performance of OD segmentation for Glaucoma affected images of HRF dataset

Image No.	Measures		
	<i>Sensitivity</i>	<i>Specificity</i>	<i>Accuracy</i>
1_g	0.9675	0.9935	0.9932
2_g	0.9810	0.9893	0.9892
3_g	0.9684	0.9978	0.9973
4_g	0.9657	0.9955	0.9951
5_g	0.7862	0.9995	0.9964
6_g	0.8921	0.9955	0.9941
7_g	0.8860	0.9950	0.9930
8_g	0.9878	0.9979	0.9978
9_g	0.9949	0.9965	0.9965
10_g	0.9987	0.9944	0.9944
11_g	0.9931	0.9971	0.9971
12_g	0.8836	0.9972	0.9957
13_g	0.9913	0.9905	0.9905
14_g	0.8083	0.9880	0.9829
15_g	0.8949	0.9952	0.9910
<b>Average</b>	<b>0.9333</b>	<b>0.9948</b>	<b>0.9936</b>

**Table 4:** Comparison of existing OD segmentation methods with the proposed method

Images	Dataset	Sensitivity	Specificity	Accuracy
Xu Zhang et al.(2019) [16]	DRIVE	0.9596	0.9989	0.9983
	DIARETDB1	0.9413	0.9984	0.9960
	DRIONS-DB	0.9531	0.9984	0.9960
Jasem Almotiri et al [17]	DRISHTI-GS	0.9313	0.9709	-
Zahoor et al [18]	HRF	0.9233	0.9892	0.9774
Gagan et al [25]	DRISHTI-GS	0.9675	0.9968	0.9959
<b>Proposed Technique</b>	<b>HRF (Health Images)</b>	<b>0.8598</b>	<b>0.9960</b>	<b>0.9927</b>
	<b>HRF (DR Images)</b>	<b>0.8582</b>	<b>0.9967</b>	<b>0.9933</b>
	<b>HRF (Glaucoma Images)</b>	<b>0.9413</b>	<b>0.9984</b>	<b>0.9960</b>

The evaluation results of OD segmentation technique with the measures of sensitivity, specificity and accuracy for the HRF database are shown in the tables Table 1-3. Table 4 has the comparison results of proposed method with the existing methods with different database. Here we achieve the high specificity and accuracy for three set images in HRF database. High accuracy denotes that this proposed method is suitable for the optic disc segmentation. Here the evaluation is done on pixel by pixel basis. When the evaluation is done on image-by-image basis, optic discs are detected correctly for all images. Thus the accuracy of this method is 100 percentage for image-by-image basis.

#### 4.2.2 Evaluation of blood vessel segmentation technique

The vessel segmentation technique is evaluated on the HRF database. Three set of images are evaluated separately with their given ground truth images and there are resulted are listed in the below tables.

**Table 5 :** Performance of vessel segmentation for healthy images of HRF dataset

Image No.	Measures		
	<i>Sensitivity</i>	<i>Specificity</i>	<i>Accuracy</i>
1_h	0.6487	0.9704	0.9574
2_h	0.7918	0.9539	0.9579
3_h	0.6660	0.9638	0.9523
4_h	0.7907	0.9882	0.9510
5_h	0.7311	0.9658	0.9543
6_h	0.7970	0.9582	0.9517
7_h	0.7568	0.9653	0.9565
8_h	0.7449	0.9574	0.9560
9_h	0.6736	0.9596	0.9571
10_h	0.6956	0.9820	0.9497
11_h	0.7827	0.9532	0.9473
12_h	0.7701	0.9534	0.9554
13_h	0.6550	0.9813	0.9578
14_h	0.7697	0.9807	0.9436
15_h	0.7421	0.9887	0.9536
<b>Average</b>	<b>0.7344</b>	<b>0.9681</b>	<b>0.9534</b>

**Table 6 :** Performance of vessel segmentation for DR affected images of HRF dataset

Image No.	Measures		
	<i>Sensitivity</i>	<i>Specificity</i>	<i>Accuracy</i>
1_dr	0.6384	0.9688	0.9529
2_dr	0.7998	0.9667	0.9583
3_dr	0.7669	0.9798	0.9561

Image No.	Measures		
	<i>Sensitivity</i>	<i>Specificity</i>	<i>Accuracy</i>
4_dr	0.6642	0.9794	0.9626
5_dr	0.6702	0.9676	0.9502
6_dr	0.7998	0.9688	0.9551
7_dr	0.6274	0.9604	0.9580
8_dr	0.7983	0.9720	0.9550
9_dr	0.6881	0.9856	0.9528
10_dr	0.7122	0.9487	0.9582
11_dr	0.7080	0.9426	0.9532
12_dr	0.6161	0.9787	0.9553
13_dr	0.7193	0.9735	0.9533
14_dr	0.7267	0.9625	0.9506
15_dr	0.7081	0.9635	0.9474
<b>Average</b>	<b>0.7096</b>	<b>0.9679</b>	<b>0.9546</b>

Table 7 : Performance of vessel segmentation for glaucoma affected images of HRF dataset

Image No.	Measures		
	<i>Sensitivity</i>	<i>Specificity</i>	<i>Accuracy</i>
1_g	0.7925	0.9712	0.9678
2_g	0.6464	0.9705	0.9679
3_g	0.7007	0.9842	0.9675
4_g	0.7070	0.9712	0.9627
5_g	0.6559	0.9695	0.9698
6_g	0.7667	0.9669	0.9606
7_g	0.7287	0.9689	0.9618
8_g	0.7537	0.9676	0.9610
9_g	0.6042	0.9720	0.9687
10_g	0.6175	0.9709	0.9686
11_g	0.7242	0.9760	0.9626
12_g	0.6927	0.9753	0.9645
13_g	0.7305	0.9713	0.9620
14_g	0.7729	0.9705	0.9629
15_g	0.7627	0.9746	0.9654
<b>Average</b>	<b>0.7104</b>	<b>0.9720</b>	<b>0.9649</b>

**Table 8:** Comparison of existing vessel segmentation methods with proposed method

Existing Methods	Healthy			DR Affected			Glaucoma Affected		
	<i>Se</i>	<i>Sp</i>	<i>Ac</i>	<i>Sn</i>	<i>Sp</i>	<i>Ac</i>	<i>Sn</i>	<i>Sp</i>	<i>Ac</i>
Odstrcilik et al (2013) [12]	0.7861	0.9750	0.9539	0.7463	0.9619	0.9445	0.7900	0.9638	0.9497
Budai et al (2013) [13]	0.662	0.992	0.961	0.658	0.977	0.955	0.687	0.986	0.965
Ramakrishnan et al (2018) [14]	0.9411	0.9534	0.952	0.7832	0.9679	0.9582	0.8419	0.9718	0.9646
<b>Proposed</b>	<b>0.7104</b>	<b>0.9720</b>	<b>0.964</b>	<b>0.7104</b>	<b>0.9720</b>	<b>0.9649</b>	<b>0.7104</b>	<b>0.9720</b>	<b>0.9649</b>

The Sensitivity, specificity and accuracy measures are calculated for each of set of HRF database and their results are tabulated in the tables Table 5-7. For every set of 15 images, their average measures are noted in the last row. These average values are compared with the existing results. This comparison measures are tabulated in the Table 8.

When compared with the existing methods, our method achieves slightly lower sensitivity, but it achieves better specificity and accuracy.

Our method is not able to segment very tiny vessels, but it segments the large blood vessels exactly. The overall accuracy of the method is higher than the existing methods.

## 5. Conclusion

Usually, retinal diseases show the symptoms in the retinal parts. Hence, the segmentation of retinal anatomical structures is necessary. In this paper, we propose a cost effective segmentation method that segment the retinal anatomical structures using simple morphological based thresholding technique. By using this technique, we segment the optic disc and retinal vessels separately. The proposed system is evaluated with the HRF database which is publicly available. For this database, the ground truth images of vessels and optic disc are given. The metrics that are used to evaluate the proposed system are sensitivity, specificity and accuracy. Since the database has three set of images such as healthy, DR affected and glaucoma affected, the evaluation is carried out for the three set of images separately for optic disc segmentation and retinal vessel segmentation. These results when compared with the existing methods are evident for the effectiveness of the proposed method in segmenting the anatomical structures with less computational task.

## References

1. J. Almotiri, K. Elleithy And A. Elleithy, 'A Multi-Anatomical Retinal Structure Segmentation System For Automatic Eye Screening Using Morphological Adaptive Fuzzy Thresholding', Ieee Journal Of Translational Engineering In Health And Medicine', Vol. 6, 2018.
2. Arjuna, R. Rose, 'Performance Analysis of Various Contrast Enhancement techniques with Illumination Equalization on Retinal Fundus Images', 2<sup>nd</sup> International Conference on Smart Systems and Inventive Technology', 2019.
3. J. Ayub, J. Ahmad, J. M. L. Aziz, S. Ayub, U. Akram, I. Basit, 'Glaucoma Detection through Optic Disc and Cup Segmentation using K-mean Clustering', 2016.
4. Budai, R. Bock, A. Maier, J. Hornegger and G. Michelson, 'Robust Vessel Segmentation in Fundus Images', International Journal of Biomedical Imaging, Vol 2013.
5. M. L. Baker, P. J. Hand, J. J. Wang, T. Y. Wong, 'Retinal Signs and Stroke Revisiting the Link Between the Eye and Brain', National Library of Medicine, 39(4):1371-9, 2008.

6. A. S. Gonzalez, D. Kaba, Y. Li, and X. Liu, 'Segmentation of the Blood Vessels and Optic Disk in Retinal Images', IEEE Journal Of Biomedical And Health Informatics, Vol. 18, No. 6, 2014.
7. Grisan et.al., 'Extraction quantitative description of vessel features in hypertensive retinopathy fundus images' in Proc. 2nd International Workshop on Computer Assisted Fundus Image Analysis, vol.6, 2001.
8. HFR Image Database: <https://www5.cs.fau.de/research/data/fundus-images/>.
9. A. Imaran et al., 'Comparative Analysis of Vessel Segmentation Techniques in Retinal Images', IEEE open access journal, volume. 7, 2019.
10. A. Kumar, P. Vashist, 'Indian community eye care in 2020: Achievements and challenges', Indian Journal of Ophthalmology, 2020.
11. S. Kumar and B. Kumar, 'Diabetic Retinopathy Detection by Extracting Area and Number of Microaneurysm from Color Fundus Image', 5<sup>th</sup> International Conference on Signal Processing and Integrated Networks, 2018.
12. Y. Lin, H. Zhang And G. Hu, 'Automatic Retinal Vessel Segmentation via Deeply Supervised and Smoothly Regularized Network', IEEE Access Journal, Vol. 7, 2019.
13. D. Lokuarachchi, L. Muthumal, K. Gunarathna, T. D. Gamage, 'Detection of Red Lesions in Retinal Images Using Image Processing and Machine Learning Techniques', Moratuwa Engineering Research Conference (MERCon) 2019.
14. J. Odstrcilik, R Kolar, A. Budai, J. Hornegger, J. Jan, J. Gazarek, T. Kubena, P. Cernosek, O. Svoboda, E. Angelopoulou, 'Retinal vessel segmentation by improved matched filtering: evaluation on a new high-resolution fundus image database', IET Image Processing, 2013.
15. S. Palanivel Rajan, 'Recognition of Cardiovascular Diseases through Retinal Images Using Optic Cup to Optic Disc Ratio', Springer Journal of Pattern Recognition and Image Analysis', Vol. 30, No. 2, 2020.
16. N. B. Prakash, D. Selvathi, and G. R. Hemalakshmi, 'Development of Algorithm for Dual Stage Classification to Estimate Severity Level of Diabetic Retinopathy in Retinal Images using Soft Computing Techniques', International Journal on Electrical Engineering and Informatics, Vol. 6, No. 4, 2014.
17. C. Raja and L. Balaji, 'An Automatic Detection of Blood Vessels in Retinal Images using Convolutional Neural Network for Diabetic Retinopathy Detection', Springer Journal of Pattern Recognition and Image Analysis', Vol. 29, No. 3, 2019.
18. Renoh et al., 'Automatic detection and segmentation of optic disc and fovea in retinal images', IET journals of Image Processing, vol. 12, Issue. 11, 2018.
19. D. A. Salz And A. J. Witkin, 'Imaging In Diabetic Retinopathy', Middle East Afr J Ophthalmol, Vol. 22, No. 2, Pp. 145-150, 2015.
20. L. Seoud, T. Hurtut, J. Chelbi, F. Cheriet, and J. M. P. Langlois, 'Red Lesion Detection Using Dynamic Shape Features for Diabetic Retinopathy Screening', IEEE Transactions on Medical Imaging, Vol.35, No. 4, 2016.
21. R. Sundaram, Ravichandran, P. Jayaraman and Venkatraman, 'Extraction of Blood Vessels in Fundus Images of Retina through Hybrid Segmentation Approach', Mathematics Journal, Vol. 7, Issue. 2, 2019.
22. K. Wisaeng And W. Sa. Ngiamvibool, 'Exudates Detection Using Morphology Mean Shift Algorithm In Retinal Images', IEEE Access Journal, Vol. 7, 2019.
23. M. N. Zahoor And M. M. Fraz, 'Fast Optic Disc Segmentation In Retina Using Polar Transform', Ieee Access Journal, Volume 5, 2017.
24. X. Zhang, J. Liu, S. Wang, Z. Chen, B. Huang, J. Ye, 'Lightweight cascade framework for optic disc Segmentation', IET Image Processing, Vol. 13 Iss. 10, pp. 1805-1810, 2019.
25. J. H. Gagan 1 , Harshit S. Shirsat2 , Yogish S. Kamath3 , Neetha I. R. Kuzhuppilly3 , And J. R. Harish Kumar, 'Automatic optic disc segmentation using basis Splines-bases Active Contour', IEEE Access, Vol, 10, pp. 88152- 88163, 2022.